SCIENTIFIC REPORTS

OPEN

SUBJECT AREAS:
NANOPHOTONICS AND PLASMONICS
ELECTRONICS, PHOTONICS AND DEVICE PHYSICS

Received
6 March 2014

Accepted
4 August 2014

Published
29 August 2014

Correspondence and requests for materials should be addressed to J.R. (jieren@mit.edu)

Non-Reciprocal Geometric Wave Diode by Engineering Asymmetric Shapes of Nonlinear Materials

Nianbei Li[1] & Jie Ren[2,3]

[1]Center for Phononics and Thermal Energy Science, School of Physics Science and Engineering, Tongji University, 200092 Shanghai, P. R. China, [2]Theoretical Division, Los Alamos National Laboratory, Los Alamos, NM 87545, USA, [3]Department of Chemistry, Massachusetts Institute of Technology, Cambridge, MA 02139, USA.

Unidirectional nonreciprocal transport is at the heart of many fundamental problems and applications in both science and technology. Here we study the novel design of wave diode devices by engineering asymmetric shapes of nonlinear materials to realize the function of non-reciprocal wave propagations. We first show analytical results revealing that both nonlinearity and asymmetry are necessary to induce such non-reciprocal (asymmetric) wave propagations. Detailed numerical simulations are further performed for a more realistic geometric wave diode model with typical asymmetric shape, where good non-reciprocal wave diode effect is demonstrated. Finally, we discuss the scalability of geometric wave diodes. The results open a flexible way for designing wave diodes efficiently simply through shape engineering of nonlinear materials, which may find broad implications in controlling energy, mass and information transports.

The pursuit of novel devices that are able to manipulate energy, mass and information transmission has stimulated huge interests in widespread physical branches such as phononics[1], photonics[2–4] and biophysics[5]. As one of the most fundamental and applicable devices, the wave diode can rectify non-reciprocal wave propagation, in analogy to electronic p-n junctions, where the transmission coefficient is significantly direction-dependent. As such, the device conducts in the forward direction but insulates in the backward one. There are many interesting theoretical proposals for thermal diodes[6–10], optical diodes[11,12], spin Seebeck diodes[13,14] and acoustic diodes[15,16], and many of them have been successfully verified by experiments[2–4,17–21].

It has been well established that linear structures are not able to break the reciprocity in reflection-transmission once the time-reversal symmetry is preserved[22]. Therefore, both nonlinearity and some kinds of symmetry breaking mechanism are essential for the real non-reciprocal propagation. In particular, the optical isolators or diodes[23] have been realized by harvesting the properties of nonlinearity and asymmetry[24–29]. The enhancement of nonreciprocal transmission via cascading has also been studied[30]. And this nonreciprocal transmission has even been achieved in PT systems[31,32]. Recently, an interesting design of wave diode is proposed[33], based on the nonreciprocal transmission in a one-dimensional (1D) nonlinear layer structure[11,12]. The model system is described by the discrete nonlinear Schrödinger (DNLS) equation, which is a reasonable approximation for the wave evolution in layered photonic or phononic crystals[34]. The spatially varying coefficients break the mirror reflection symmetry and this non-homogeneity generates the asymmetric wave propagation together with nonlinearity. However, the inhomogeneity of coefficients is not the only way to achieve non-reciprocal wave propagation and also it is usually very hard to design the inhomogeneous coefficient in real materials.

To circumvent the difficulty, in this article we report another novel design by seeking the symmetry breaking from pure geometric point of view, i.e, engineering asymmetric shapes of homogenous materials. The advantage of utilizing geometric asymmetry is guaranteed by the easy and convenient fabrication of functional devices merely through shape engineering. Different functionality can thus be tunable by simply tailored adjusting of the geometric shape of the target device. Therefore, the design of a wave diode device purely induced by geometric effect is very important in the practical point of view and would have found potential applications in the future.

To unraveling the underlying mechanism of the nonreciprocal geometric wave diode, we first analytically solve the transmission problem for a simple model, where the functional nonlinear part consists of a triangle structure coupled to a linear ladder lattice in the left and a linear 1D chain in the right. The derived transmission coefficients exhibit clear asymmetry depending on the direction of the incident wave, thanks to the nonlinear triangle structure. The strength and sign of the non-reciprocity can also be tuned by the intensity of the incident wave. We then investigate a more realistic system with typical asymmetric geometry. The system is complicated and

analytical result is no longer available so that we resort to intensive numerical simulations of the propagation of wave packets. The results clearly demonstrate non-reciprocal wave propagations induced by the asymmetric geometry of nonlinear materials. We further verify that our proposed wave diode devices will not change the frequency of the incident wave packet which would be important in practical applications. Finally, we discuss the scalability of the geometric wave diode.

Results

Analytic results for a simple geometric diode. Figure 1(a) shows the sketch of a simple geometric wave diode model with non-reciprocal wave transmission induced by asymmetric shape. The central triangle lattice with $L_c = 2$ interfacial layers is made of nonlinear materials and plays the role of functionality for the device. The nonlinear triangle is then coupled with semi-infinite linear ladder lattice in the left and 1D linear chain in the right, respectively.

The evolution of wave amplitude ψ_l at each site l follows the time-dependent DNLS equation[35]:

$$i\dot{\psi}_l = (U_l + n_l)\psi_l + g_l|\psi_l|^2\psi_l - \sum_{m_l}\psi_{m_l} \tag{1}$$

where U_l and n_l depict the on-site energy and the number of nearest-neighbors of site l, g_l is the nonlinear strength and m_l denotes the index of nearest-neighbors of site l. The on-site energy and nonlinear strength have homogeneous non-zero values $U_l = U$ and $g_l = g$ only in the central functional part. Therefore the symmetry breaking only comes from the geometry. For the right 1D linear chain, the dispersion relation can be obtained as $\omega = 2 - 2\cos k_R$, where the plane wave solution has the form of $\psi_l = A_l e^{-i(\omega t - k_R l)}$. While for the left linear ladder, there are two branches for the energy band. Depending on whether bilateral amplitudes on the ladder are (anti-)symmetric $\psi_{l'} = \pm\psi_l$ where l' denotes the site in the lower chain of the left ladder, the dispersion relations of the plane wave solutions are $\omega = 2 - 2\cos k_L$ and $\omega = 4 - 2\cos k_L$, respectively.

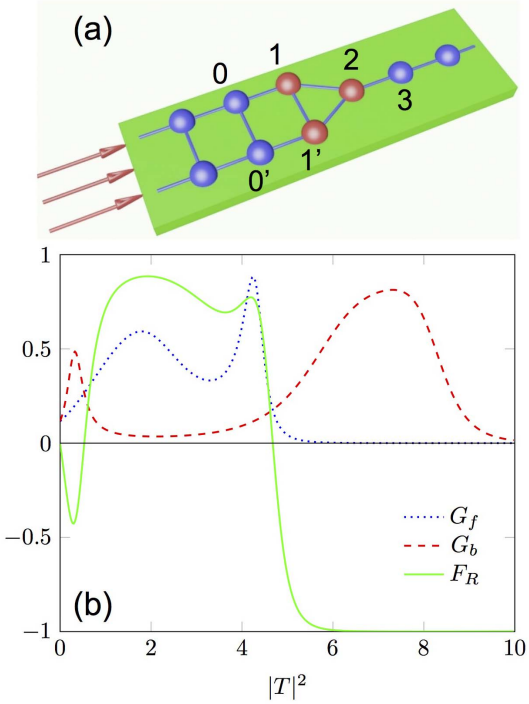

Figure 1 | (a) Sketch of the geometric wave diode. The central $L_c = 2$ interfacial layers are nonlinear, with asymmetric geometry. Its left is coupled with a semi-infinite linear ladder lattice. The right is connected to a semi-infinite 1D linear lattice. The linear structures are free of on-site potentials and the central 2 layer interfaces are with identical nonlinear strength g and on-site potential U. The arrows schematically denote the forward incident direction. (b) Transmission coefficients and rectification factor as a function of the intensity of transmitted waves. The wave vectors are identical with $k = 1.57$ for both left and right incoming waves. The on-site energy $U = -3.5$ and nonlinear strength $g = 1$ are set for the central two layers.

We can analytically solve the transmission problem of the wave propagation by the scattering approach similar as in Ref. [33]. For the incident wave coming from left to right, the solutions of the wave amplitudes in the central four layers [see Fig. 1(a)] can be expressed with the following boundary conditions:

$$\begin{aligned} &\psi_0 = \psi_{0'} = I + R, \quad && \psi_1 = \psi_{1'} = Ie^{ik_L} + Re^{-ik_L} \\ &\psi_2 = Te^{ik_R}, && \psi_3 = \psi_2 e^{ik_R} \end{aligned} \tag{2}$$

where I, R and T denote incident, reflected and transmitted wave amplitudes, respectively. Without loss of generality, we only consider the lower dispersion branch of the left ladder lattice, which is identical to that of the right 1D chain by assuming $\psi_{l'} = \psi_l$. As such, both left and right linear structures have the same dispersion and the wave vectors are identical with $k_{L,R} = k$ under the same energy. Therefore, the forward transmission coefficient G_f (where subscript f denotes forward) from left to right can be derived as the function of transmitted wave intensity $|T|^2$ (see Methods for the detailed derivation):

$$G_f := \frac{|T|^2 \sin k_R}{2|I|^2 \sin k_L} = \frac{8\sin k_L \sin k_R}{|2-(\alpha - e^{ik_L})(\beta - e^{ik_R})|^2} \tag{3}$$

where $\beta \equiv U + 3 - \omega + g|T|^2$ and $\alpha \equiv U + 2 - \omega + g|T|^2(\beta^2 + 1 - 2\beta\cos k_R)/4$. The ratio $\sin k_R/\sin k_L$ appears in the definition as a renormalization factor because the group velocities of incident waves of the left and right leads might not be the same (if the upper energy branch of the left side is chosen, in our case). The factor 2 in the denominator is the consequence that there are two incident channels from the left due to the ladder structure. One can readily verify the conservation condition $2|I|^2 \sin k_L = 2|R|^2 \sin k_L + |T|^2 \sin k_R$. In the same manner, the backward transmission coefficient G_b (where subscript b denotes backward) from right to left can also be obtained as:

$$G_b := \frac{2|T_b|^2 \sin k_L}{|I_b|^2 \sin k_R} = \frac{8\sin k_L \sin k_R}{|2-(\alpha_b - e^{ik_L})(\beta_b - e^{ik_R})|^2} \tag{4}$$

with $\alpha_b \equiv U + 2 - \omega + g|T_b|^2$ and $\beta_b \equiv U + 3 - \omega + g|T_b|^2(\alpha_b^2 + 1 - 2\alpha_b\cos k_R)$. One can also readily verify the conservation in the backward direction that $|I_b|^2 \sin k_L = |R_b|^2 \sin k_L + 2|T_b|^2 \sin k_R$. The factor 2 is due to the fact that there are two transmitted channels to the left.

Although the forward and backward transmission coefficients G_f and G_b have similar expressions, the non-identical behavior between parameters (α, β) and (α_b, β_b) implies the existence of direction-dependent transmission coefficients. For plane waves with same intensities, the incident waves will be scattered differently by the central nonlinear triangle due to its asymmetric shape in respect to the forward and backward waves, which leads to the non-reciprocal propagation. To quantify the magnitude of the non-reciprocity, a rectification factor F_R can be defined as:

$$F_R = \frac{G_f - G_b}{G_f + G_b} \tag{5}$$

where a non-zero value of F_R emerges for the non-reciprocal wave propagation and reaches to its maximal asymmetry with values $F_R = \pm 1$.

We plot G_f and G_b as well as F_R in Fig. 1(b), as a function of the transmitted wave intensities $|T|^2 = 2|T_b|^2$ according to Eq. (3) and (4). (Note here, we choose the same transmitted intensities for the convenience, because the transmission is analytically expressed in

terms of transmitted intensities. We have checked at the stable regime that the same incident amplitudes also produce the nonreciprocal transmission. In fact, in the following simulations, we choose transmissions at the same incident amplitudes for the comparison.) We can see that the dependence of G_f and G_b on transmitted intensities are almost opposite to each other. As a result, significant nonreciprocal effect of wave propagation emerges and the rectification factor F_R can even change its sign as the modulation of transmitted wave intensities. We would like to remark that analytically we obtain the nonreciprocal transmission because $\alpha \neq \alpha_b$, $\beta \neq \beta_b$ that are consequences of both the nonlinearity and the asymmetric geometry. If the shape is symmetric, we of course have symmetric transmissions. If the nonlinearity vanishes $g \to 0$, even with keeping the asymmetric geometry, we can see analytically that $\alpha = \alpha_b$ and $\beta = \beta_b$ so that the reciprocal transmissions are also recovered.

Simulation results for a more realistic geometric diode. We now consider a more realistic model with typical asymmetric geometry displayed in Fig. 2(a). The central functional part with layer index $1 \leq l \leq L_c$ is nonlinear in nature and has asymmetric shape. The same left and right linear ladder lattices are coupled with the central part. The system is too complicated to be tackled analytically. Therefore, numerical simulations will be performed to investigate the wave propagation in such a setup.

We consider the propagation of a pulse or say a Gaussian wave packet with the initial condition:

$$\psi_l(t=0) = Ie^{-\left(\frac{l-l_0}{d}\right)^2 + ikl} \tag{6}$$

where d and l_0 is the width and central position of the wave packet, respectively. The numerical transmission coefficients G_f and G_b are defined as the sum of transmitted density norms $\sum_{l>L_c} |\psi_l(t)|^2$ at the end of time evolution normalized by the sum of initial density norms $\sum_{l<1} |\psi_l(t=0)|^2$. In Fig. 2(b), we plot the numerical forward and backward transmission coefficients G_f and G_b as well as the numerical F_R as a function of incident wave intensities $|I|^2$. Although the profiles of forward and backward transmission coefficients exhibit similar behaviors, a lag between them is enough to give rise to a profound non-reciprocal wave diode effect.

Figure 3(a,b) displays typical examples of time evolution for the same initial wave packets with opposite incident directions. In the forward direction, most of the incident waves have been reflected by the nonlinear central part. While in the backward direction, most of the incident waves can pass through the nonlinear central part. Accordingly, figure 3(c,d) shows the distinct density distributions within the nonlinear triangular part for forward and backward wave transmissions, respectively. The snapshots evidence that the forward wave is blocked at the smaller end of the triangle when the wave is incident from the left to the right, while the backward wave successfully passes through the central part when incident from the larger end of the triangle (right) to the smaller one (left). The interplay between nonlinearity and asymmetric geometry within the central functional part yields the non-reciprocal wave propagations. The asymmetric behavior can be modulated by the incident wave intensities and wave vector k. More importantly, the sign and magnitude of this non-reciprocity can also be manipulated by the geometric shape of the central part. Further, to check whether the frequency of the wave packet can be shifted or not after the scattering, we plot the power spectra of the wave packet at the end of time evolution in Fig. 3(e,f). Although nonlinear resonances can be generated by the central part, the reflected and transmitted wave packets almost maintain their original frequencies. This effect is important for many practical applications since usually we do want to retain the frequency of the original signal after it passes through the functional devices.

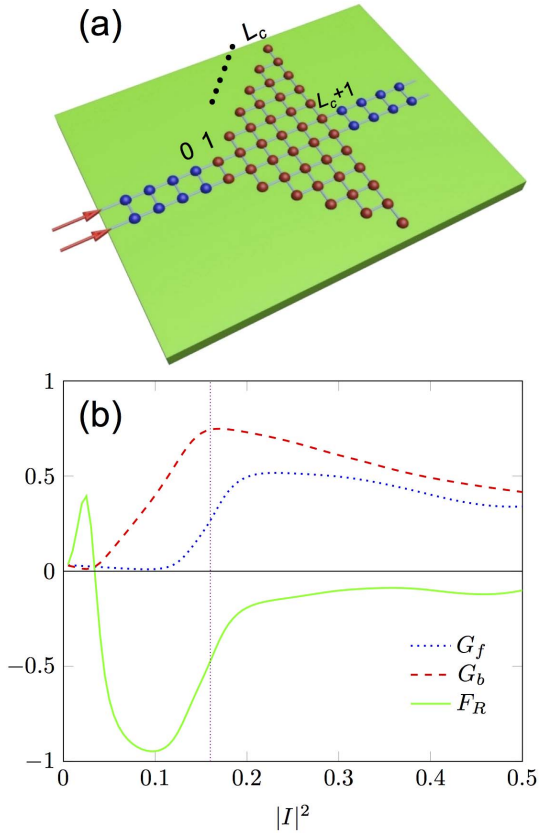

Figure 2 | (a) Sketch of a more realistic geometric wave diode. The central L_c layers are nonlinear, with asymmetric shape. The left and right are coupled with the same semi-infinite linear ladder lattices. The linear structures are free of on-site potentials and the central layers are with homogeneous nonlinear strength g and on-site potential U. The arrows schematically denote the forward incident direction. (b) Transmission coefficients and rectification factor as a function of the intensity of incident waves. The initial wave intensities are the same for both directions with $|I|^2 = |I_b|^2$. The absolute values of wave vectors are identical with $|k| = 1.57$ for both left and right incident waves. The central part has $L_c = 6$ layers with homogeneous on-site energy $U = 1$ and nonlinear strength $g = 1$. Both of the left and right linear ladders have $L_l = L_r = 500$ layers. The width of the initial wave packet is $d = 100$ and the central position of the initial wave packet is $l_0 = 250$ (750) for left (right) incident wave. The vertical line denotes the initial wave intensities $|I|^2$ used in Fig. 3.

Finally, we discuss the scalability of the rectifying function of geometric wave diodes by linking them in series. As shown in Fig. 4, when scaling up to multiple diodes, the rectification is enhanced. This can be understood by the following very rough but intuitive reasoning: Assuming n geometric diodes in series are independent and not interact with each other, then their forward transmission coefficient is n times multiplication of the singe one, expressed as G_f^n. Accordingly, their backward transmission coefficient will be G_b^n. As such, the total rectification factor for the n geometric diodes expresses as $F_R^n = \left(1 - \left(\frac{G_b}{G_f}\right)^n\right) \Big/ \left(1 + \left(\frac{G_b}{G_f}\right)^n\right)$. Readily, it can be proved that increasing n will always enhance F_R^n to its extremum values $\pm$ 1. However, this is just a rough estimation for ideal cases. In reality, the situation is more complicated: the enhancement of the rectification will saturate at some optimal number (5 in Fig. 4), or decrease, or even reverse the sign, depending on the wave vector k and intensities (not shown). More importantly, scaling up the diode devices will steadily suppress the transmission since its value is always smaller than 1, i.e., G^n decreases with n since $G < 1$ generally. Therefore, in

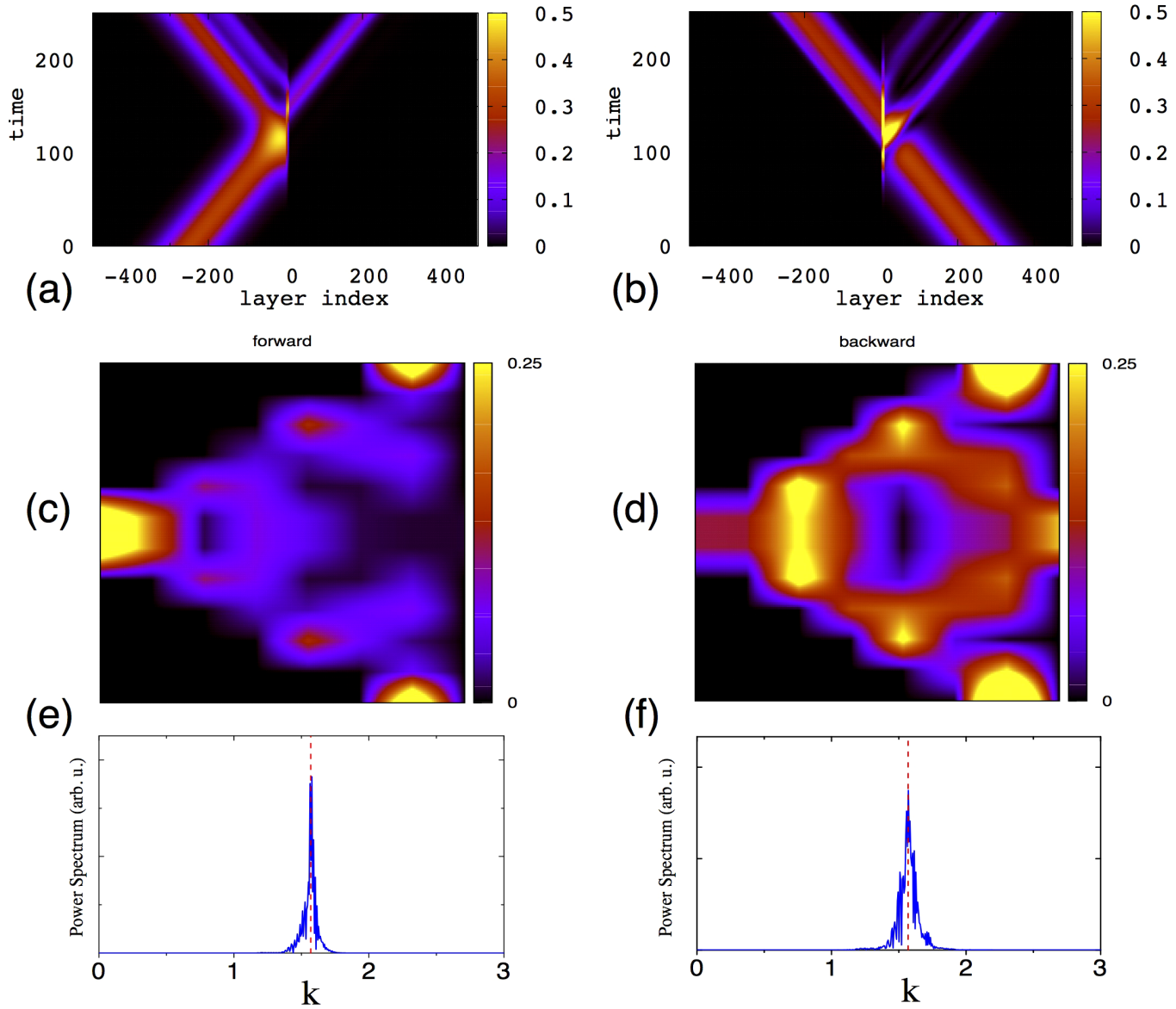

Figure 3 | (a,b) Time evolution of left and right incoming Gaussian wave packets demonstrates the device as a wave diode. The parameter setup is the same as in Fig. 2 with the initial wave intensities $|I|^2 = 0.16$ as marked by the vertical line there. (c,d) The density distributions within the triangular part for forward and backward cases, respectively. The snapshots are taken at the time when the center of the wave packet is traveling to the inside of the triangular part. (e,f) Power spectra of the real part of ψ_l at the ending time of the evolution for left and right incoming wave packets, respectively. The initial wave vectors are $|k| = 1.57$, represented by the vertical dotted lines in left and right panels. The ending time of the evolution is $t = 253$.

practice, one need find the optimal number of geometric wave diodes to balance demand of both the transmission and the rectification.

Discussion

Geometric phonon and electron diodes have been studied both theoretically and experimentally[38–43]. However, to our best knowledge so far there is no existing exact results to clearly expose the underlying physics, especially for the more general geometric "wave" diode, before this work. In particular, the role of nonlinearity (many-body interaction beyond quadric order) to the geometric diode has not been appreciated.

Therefore, it is worthwhile to emphasize here that the asymmetry alone in linear (quadric) systems cannot induce non-reciprocal wave propagation. Asymmetry must come to play together with nonlinearity to give rise to non-reciprocal wave diodes. In all our studied systems, we have either analytically or numerically checked that the effect of non-reciprocal wave propagation will totally disappear if the nonlinearity is tuned to be zero while keeping all other asymmetric settings. These would explain why the electric and thermal rectifications measured in the asymmetric graphene and its oxide systems are too low[40,42] [both are below 0.13 according to our Eq. (5)], because in these graphene-related systems electrons and phonons are weakly interacting (especially at low temperatures) so that the nonlinearity (high order many-body interaction) is nearly absent. To observe the significant rectification in those systems, one need go to the high temperature regime, where the nonlinear effect due to many-body interactions can be enhanced. (Note that extremely low temperature can also produce and enhance the nonlinear effect due to many-body interactions, e.g., the nonlinear term in the Gross-Pitaevskii equation for Bose-Einstein Condensates.)

The interplay between some kind of symmetry breaking mechanism and nonlinearity is essential to realizing non-reciprocal wave

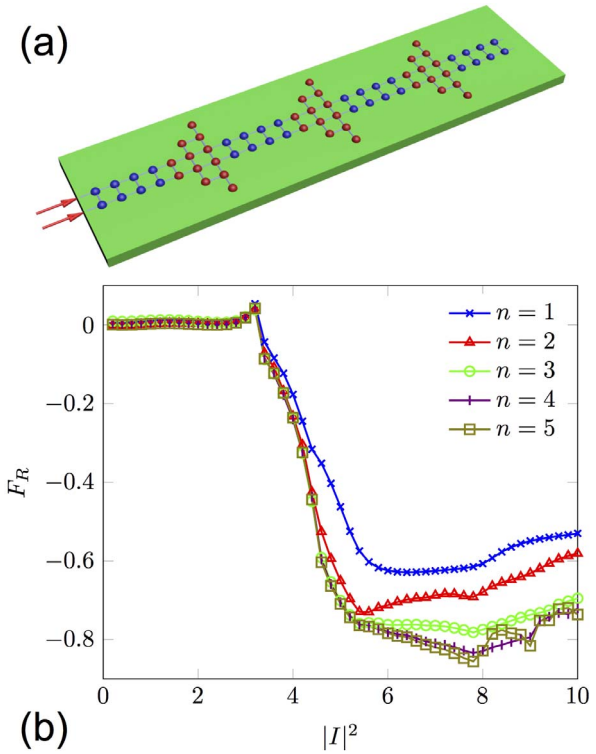

Figure 4 | (a) Sketch of a geometric wave diode linked in series. The n diodes ($n = 3$ in the sketch) are linked in series to enhance the rectification factor. The arrows schematically denote the forward incident direction. (b) Rectification factor as a function of the number of diodes linked in series. The central part for each diode has $L_c = 3$ nonlinear layers with homogeneous on-site energy $U = -1$ and nonlinear strength $g = 0.1$. The linear ladder between neighboring diodes has $L_{ll} = 50$ layers and the most left and right linear ladders has $L_l = L_r = 1000$ layers. The wave vectors and width of initial wave packets are $|k| = 0.8$ and $d = 30$, respectively. The central positions of the initial wave packets are in a distance of 250 layers to the nearest end and the ending time is determined when the travelling distance of the central peak equals to $L - 500$ where L is the total number of layers of the whole system.

propagation. Ref. [33] breaks the symmetry by setting spatially varying inhomogenous coefficients to induce asymmetric propagation. Here we proposed a novel design of the so called geometric wave diode by tailoring the asymmetric shape of the central functional part of the device. The functional nonlinear part of asymmetric shape can be conveniently fabricated in practice and easily be replaced by other shapes with different or even reversed rectifications. Therefore, the most manipulability of the non-reciprocal wave propagation can be solely achieved by geometry engineering of the central functional part.

In conclusion, we have shown the non-reciprocal geometric wave diode by engineering asymmetric shapes of nonlinear materials. For a simple model, we have obtained analytical results, which explicitly prove that the non-reciprocal wave propagation can be induced by the asymmetric shape in nonlinear materials. We then have performed numerical simulations to study a more realistic diode model with typical geometric asymmetry. Profound non-reciprocal propagations of wave packets have been verified with tailored design of interplay between nonlinearity and geometric asymmetry. Most importantly, the sign and magnitude of the non-reciprocity of the wave propagation can be manipulated by shaping the central functional part into different geometric structures.

Since the DNLS has found widespread implications in optics, cold atoms and spin electronics, the proposed design in this article might also find its applications in controlling the light propagation in nonlinear optical wave guides, cold atom transport in atomtronics[44,45], or spin wave transport in spin caloritronics[14]. In the future, it would be interesting to explore how the asymmetric geometry optimizes the rectification of energy, mass or information transmission, which may have a deep connection to the quantum chaos[46] with nonlinearity.

Methods

In order to analytically solve the transmission problem for the first model, we find the traveling wave solution of $\psi_l \sim e^{-i\omega t}$ for Eq. (1) as:

$$\omega\psi_l = (U_l + n_l)\psi_l + g_l|\psi_l|^2\psi_l - \sum_{m_l}\psi_{m_l} \tag{7}$$

Apply the above equation to site 2 in Model I, we obtain:

$$\omega\psi_2 = (U+3)\psi_2 + g|\psi_2|^2\psi_2 - (\psi_1 + \psi_{1'} + \psi_3) \tag{8}$$

it can be regrouped by knowing that $\psi_1 = \psi_{1'}$ and $\psi_3 = e^{ik_R}\psi_2$ from the boundary conditions of Eq. (2):

$$\psi_1 = \frac{1}{2}(\beta - e^{ik_R})\psi_2 \tag{9}$$

with

$$\beta = U + 3 - \omega + g|T|^2 \tag{10}$$

Apply Eq. (7) to site 1, we obtain:

$$\omega\psi_1 = (U+3)\psi_1 + g|\psi_1|^2\psi_1 - (\psi_0 + \psi_{1'} + \psi_2) \tag{11}$$

After regrouping and substitution we can obtain:

$$\psi_0 = \left(\frac{1}{2}\alpha(\beta - e^{ik_R}) - 1\right)\psi_2 \tag{12}$$

with

$$\alpha = U + 2 - \omega + g|T|^2(\beta^2 + 1 - 2\beta\cos k_R)/4 \tag{13}$$

From the first two boundary conditions in Eq. (2), the incident amplitude I can be expressed as:

$$I = \frac{e^{-ik_L}\psi_0 - \psi_1}{e^{-ik_L} - e^{ik_L}} \tag{14}$$

Substitute the expression of ψ_0 and ψ_1 into above formula and noticing that $\psi_2 = Te^{ik_R}$ in Eq. (2), we can obtain the relation between incident and transmitted amplitude:

$$I = e^{ik_R}\frac{e^{-ik_L}(\alpha(\beta - e^{ik_R})/2 - 1) - (\beta - e^{ik_R})/2}{e^{-ik_L} - e^{ik_L}}T \tag{15}$$

The transmission coefficient of Eq. (3) can thus be derived analytically. For the reversed direction, the transmission coefficient of Eq. (4) can also be derived with the same consideration.

For the numerical simulation, we apply the symplectic PQ method introduced in the appendix of Ref. [36] to integrate the time dependent DNLS equations. It is a $SBAB_2$ based symplectic algorithm[37]. The dimensionless time step $\Delta t = 0.02$ has been used in all the numerical simulations.

1. Li, N. *et al.* Colloquium: Phononics: Manipulating heat flow with electronic analogs and beyond. *Rev. Mod. Phys.* **84**, 1045 (2012).
2. Hwang, J. *et al.* Electro-tunable optical diode based on photonic bandgap liquid-crystal heterojunctions. *Nat. Materials* **4**, 383 (2005).
3. Yu, Z. & Fan, S. Complete optical isolation created by indirect interband photonic transitions. *Nat. Photonics* **3**, 91 (2009).
4. Fan, L. *et al.* An All-Silicon Passive Optical Diode. *Science* **335**, 447 (2011).
5. Hanggi, P. & Marchesoni, F. Artificial Brownian motors: Controlling transport on the nanoscale. *Rev. Mod. Phys.* **81**, 387 (2009).
6. Terraneo, M., Peyrard, M. & Casati, G. Controlling the Energy Flow in Nonlinear Lattices: A Model for a Thermal Rectifier. *Phys. Rev. Lett.* **88**, 094302 (2002).
7. Li, B., Wang, L. & Casati, G. Thermal Diode: Rectification of Heat Flux. *Phys. Rev. Lett.* **93**, 184301 (2004).
8. Li, B., Lan, J. H. & Wang, L. Interface Thermal Resistance between Dissimilar Anharmonic Lattices. *Phys. Rev. Lett.* **95**, 104302 (2005).
9. Hu, B., Yang, L. & Zhang, Y. Asymmetric Heat Conduction in Nonlinear Lattices. *Phys. Rev. Lett.* **97**, 124302 (2006).
10. Otey, C. R., Lau, W. T. & Fan, S. Thermal Rectification through Vacuum. *Phys. Rev. Lett.* **104**, 154301 (2010).
11. Konotop, V. V. & Kuzmiak, V. Nonreciprocal frequency doubler of electromagnetic waves based on a photonic crystal. *Phys. Rev. B* **66**, 235208 (2002).

12. Tocci, M. D. *et al.* Thin-film nonlinear optical diode. *Appl. Phys. Lett.* **66**, 2324 (1995).
13. Ren, J. Predicted rectification and negative differential spin Seebeck effect at magnetic interfaces. *Phys. Rev. B* **88**, 220406(R) (2013).
14. Ren, J. & Zhu, J.-X. Theory of asymmetric and negative differential magnon tunneling under temperature bias: Towards a spin Seebeck diode and transistor. *Phys. Rev. B* **88**, 094427 (2013).
15. Mathur, S. S. & Sago, M. S. Rectification of acoustic waves. *Can. J. Phys.* **52**, 1726 (1974).
16. Liang, B., Yuan, B. & Cheng, J.-c. Acoustic Diode: Rectification of Acoustic Energy Flux in One-Dimensional Systems. *Phys. Rev. Lett.* **103**, 104301 (2009).
17. Chang, C. W., Okawa, D., Majumdar, A. & Zettl, A. Solid-state thermal rectifier. *Science* **314**, 1121 (2006).
18. Bender, N. *et al.* Observation of Asymmetric Transport in Structures with Active Nonlinearities. *Phys. Rev. Lett.* **110**, 234101 (2013).
19. Liang, B. *et al.* An acoustic rectifier. *Nat. Materials* **9**, 989 (2010).
20. Boechler, N., Theocharis, G. & Daraio, C. Bifurcation-based acoustic switching and rectification. *Nat. Materials* **10**, 665 (2011).
21. Li, X.-F. *et al.* Tunable Unidirectional Sound Propagation through a Sonic-Crystal-Based Acoustic Diode. *Phys. Rev. Lett.* **106**, 084301 (2011).
22. Beenakker, C. W. J. Random-matrix theory of quantum transport. *Rev. Mod. Phys.* **69**, 731 (1997).
23. Jalas, D. *et al.* What is - and what is not - an optical isolator. *Nat. Photonics* **7**, 579 (2013).
24. Gallo, K. *et al.* All-optical diode in a periodically poled lithium niobate waveguide. *Appl. Phys. Lett.* **79**, 314 (2001).
25. Alberucci, A. & Assanto, G. All-optical isolation by directional coupling. *Opt. Lett.* **33**, 1641 (2008).
26. Rao, V. S. C., Manga Gupta, Dutta, S. & Agarwal, G. S. Study of asymmetric multilayered structures by means of nonreciprocity in phases. *J. Opt. B* **6**, 555 (2004).
27. Kumari, M. & Gupta, S. Dutta. Positive and negative giant Goos-Hänchen shift in a near-symmetric layered medium for illumination from opposite ends. *Opt. Commun.* **285**, 617 (2012).
28. Fratalocchi, A. & Assanto, G. Symmetry-breaking instabilities in perturbed optical lattices: Nonlinear nonreciprocity and macroscopic self-trapping. *Phys. Rev. A* **75**, 063828 (2007).
29. Miroshnichenko Andrey, E., Brasselet, E. & Kivshar Yuri, S. Reversible optical nonreciprocity in periodic structures with liquid crystals. *Appl. Phys. Lett.* **96**, 063302 (2010).
30. Galland, C. *et al.* Broadband on-chip optical non-reciprocity using phase modulators. *Opt. Expr.* **21**, 14500 (2013).
31. Rüter Christian, E. *et al.* Observation of parity-time symmetry in optics. *Nat. Phys.* **6**, 192 (2010).
32. Liu, X., Gupta Subhasish, D. & Agarwal, G. S. Regularization of the spectral singularity in PT-symmetric systems by all-order nonlinearities: Nonreciprocity and optical isolation. *Phys. Rev. A* **89**, 013824 (2014).
33. Lepri, S. & Casati, G. Asymmetric Wave Propagation in Nonlinear Systems. *Phys. Rev. Lett.* **106**, 164101 (2011).
34. Kosevich, A. M. & Mamalui, M. A. Linear and nonlinear vibrations and waves in optical or acoustic superlattices (photonic or phonon crystals). *J. Exp. Theor. Phys.* **95**, 777 (2002).
35. Hennig, D. & Tsironis, G. P. Wave transmission in nonlinear lattices. *Phy. Rep.* **307**, 333 (1999).
36. Bodyfelt, B. D., Laptyeva, T. V., Skokos, Ch., Krimer, D. O. & Flach, S. Nonlinear waves in disordered chains: Probing the limits of chaos and spreading. *Phys. Rev. E* **84**, 016205 (2011).
37. Laskar, J. & Robutel, P. High order symplectic integrators for perturbed Hamiltonian systems. *Celest. Mech. Dyn. Astron.* **80**, 39 (2001).
38. Yang, N., Zhang, G. & Li, B. Carbon nanocone: A promising thermal rectifier. *Appl. Phys. Lett.* **93**, 243111 (2008).
39. Hu, J., Ruan, X. & Chen, Y.-P. Thermal Conductivity and Thermal Rectification in Graphene Nanoribbons: A Molecular Dynamics Study. *Nano Lett.* **9**, 2730 (2009).
40. Tian, H. *et al.* A Novel Solid-State Thermal Rectifier Based On Reduced Graphene Oxide. *Sci. Rep.* **2**, 523 (2012).
41. Choi, K. *et al.* Geometry enhanced asymmetric rectifying tunneling diodes. *J. Vac. Sci. Technol. B* **28**, C6O50 (2010).
42. Dragoman, D. & Dragoman, M. Geometrically induced rectification in two-dimensional ballistic nan-odevices. *J. Phys. D: Appl. Phys.* **46**, 055306 (2013).
43. Zhu, X., Joshi, S., Grover, S. & Moddel, G. Graphene geometric diodes for terahertz rectennas. *J. Phys. D: Appl. Phys.* **46**, 185101 (2013).
44. Seaman, B. T., Krämer, M., Anderson, D. Z. & Holland, M. J. Atomtronics: Ultracold-atom analogs of electronic devices. *Phys. Rev. A* **75**, 023615 (2007).
45. Pepino, R. A., Cooper, J., Anderson, D. Z. & Holland, M. J. Atomtronic Circuits of Diodes and Transistors. *Phys. Rev. Lett.* **103**, 140405 (2009).
46. Ni, X., Huang, L., Lai, Y.-C. & Grebogi, C. Scarring of Dirac fermions in chaotic billiards. *Phys. Rev. E* **86**, 016702 (2012).

Acknowledgments

N.L. acknowledges the supports from Shanghai Supercomputer Center, the National Natural Science Foundation of China, Grant No. 11205114, and Shanghai Rising-Star Program with Grant No. 13QA1403600. J.R. thanks the support by the National Nuclear Security Administration of the U.S. DOE at LANL under Contract No. DE-AC52-06NA25396 through the LDRD Program. Jie is also partially supported by the Center for Excitonics (MIT) funded by the US Department of Energy, Office of Basic Energy Sciences (DE-SC0001088).

Author contributions

The present research stemmed from fruitful discussions between N.L. and J.R. Both authors N.L. and J.R. contributed to the writing of the manuscript.

Additional information

Competing financial interests: The authors declare no competing financial interests.

How to cite this article: Li, N. & Ren, J. Non-Reciprocal Geometric Wave Diode by Engineering Asymmetric Shapes of Nonlinear Materials. *Sci. Rep.* **4**, 6228; DOI:10.1038/srep06228 (2014).

This work is licensed under a Creative Commons Attribution-NonCommercial-ShareAlike 4.0 International License. The images or other third party material in this article are included in the article's Creative Commons license, unless indicated otherwise in the credit line; if the material is not included under the Creative Commons license, users will need to obtain permission from the license holder in order to reproduce the material. To view a copy of this license, visit http://creativecommons.org/licenses/by-nc-sa/4.0/